Algorithm Development for a Real-Time Military Noise Monitor

Final Report
SI-1436

Dr. Jeffrey S. Vipperman
Brian Bucci

University of Pittsburgh
Department of Mechanical Engineering
648 Benedum Hall
Pittsburgh, PA 15261

March 24, 2006

Report Documentation Page

Public reporting burden for the collection of information is estimated to average 1 hour per response, including the time for reviewing instructions, searching existing data sources, gathering and maintaining the data needed, and completing and reviewing the collection of information. Send comments regarding this burden estimate or any other aspect of this collection of information, including suggestions for reducing this burden, to Washington Headquarters Services, Directorate for Information Operations and Reports, 1215 Jefferson Davis Highway, Suite 1204, Arlington VA 22202-4302. Respondents should be aware that notwithstanding any other provision of law, no person shall be subject to a penalty for failing to comply with a collection of information if it does not display a currently valid OMB control number.

1. REPORT DATE **24 MAR 2006**	2. REPORT TYPE **Final**	3. DATES COVERED **-**

4. TITLE AND SUBTITLE	5a. CONTRACT NUMBER
Algorithm Development for a Real Time Military Noise Monitor	5b. GRANT NUMBER
	5c. PROGRAM ELEMENT NUMBER
6. AUTHOR(S) **Jeffrey Vipperman Brian Bucci**	5d. PROJECT NUMBER **SI-1436**
	5e. TASK NUMBER
	5f. WORK UNIT NUMBER

7. PERFORMING ORGANIZATION NAME(S) AND ADDRESS(ES) **University of Pittsburgh 648 Benedum Hall 3700 O'Hara Street Pittsburgh, PA 15261**	8. PERFORMING ORGANIZATION REPORT NUMBER

9. SPONSORING/MONITORING AGENCY NAME(S) AND ADDRESS(ES) **Strategic Environmental Research & Development Program 901 North Stuart Street, Suite 303 Arlington, VA 22203**	10. SPONSOR/MONITOR'S ACRONYM(S) **SERDP**
	11. SPONSOR/MONITOR'S REPORT NUMBER(S)

12. DISTRIBUTION/AVAILABILITY STATEMENT
Approved for public release, distribution unlimited

13. SUPPLEMENTARY NOTES

14. ABSTRACT

15. SUBJECT TERMS

16. SECURITY CLASSIFICATION OF:			17. LIMITATION OF ABSTRACT	18. NUMBER OF PAGES	19a. NAME OF RESPONSIBLE PERSON
a. REPORT **unclassified**	b. ABSTRACT **unclassified**	c. THIS PAGE **unclassified**	**UU**	**37**	

Table of Contents

List of Figures

List of Tables

List of Acronyms

ADC	Analog to Digital Converter
ANN	Artificial Neural Network
BLAM	Blast Analysis and Monitoring System
B&K	Bruel and Kjaer
CD	Compact Disc
CF	Crest Factor
DSP	Digital Signal Processing
Dur	Duration
ESLM	Enhanced Sound Level Meter
ERDC-CERL	Engineer Research and Development Center/Construction Engineering Research Laboratory
FFT	Fast Fourier Transform
FTIG	Fort Indiantown Gap
Kurt	Kurtosis
LD	Larson Davis
L_{eq}	Equivalent Sound Level
L_{8eq}	8-hr Equivalent Sound Level
L_{pk}	Peak Sound Level
m	Spectral Slope
MCBCL	Marine Corps Base Camp Lejeune
Neg	Number of negative samples
NI	National Instruments
Pos	Number of positive samples
PSD	Power Spectral Density
SEL	Sound Exposure Level
SERDP	Strategic Environmental Research and Development Program
SEED	SERDP Exploratory Development
SLM	Sound Level Meter
USA-CHPPM	US Army Center for Health Promotion and Preventive Medicine
S/N	Signal to Noise Ratio
VI	Virtual Instrument
WSE	Weighted Square Error

Acknowledgements

Executive Summary

The long-range goal of this 1-year SERDP Exploratory Development (SEED) project was to create an improved real-time, high-energy military impulse noise monitoring system that can detect events with peak levels (L_{pk}) as low as 100 dB with a high degree of accuracy and post the results in readily usable format. Toward this goal, this phase of the project was concerned with field data collection of noise measurements to support algorithm development, processing of the signals with software to extract standard signal metrics, development of new metrics that would improve classification accuracy, and the development, training and evaluation of an artificial neural network (ANN) that used the signal metrics to determine whether a particular noise source was military impulse noise or not. Current noise monitors suffer from inaccuracies since they look for a particular shape in the noise waveform, which can be highly variable. It is reported that detection of signals with L_{pk} below 115 dB is difficult or impossible and that false positives (as high as 10%) can occur (primarily from wind triggers) [SERDP, 2003].

Data collection trips were conducted to the US Marine Corps Base Camp Lejeune (MCBCL), NC (military and wind noise sources), Fort Indiantown Gap (FTIG), PA (military and wind noise sources), central Ohio (wind noise source) and suburban Pittsburgh (wind noise source). These data collection trips yielded approximately 1,000 usable waveforms (330 military impulse and 670 non-impulse events). A custom data collection system was assembled from various pieces of hardware and software to permit the collection of intermittent (impulse) or continuous (wind) sampling of signals. The data collected by this system was subsequently processed by an code developed at the University of Pittsburgh to extract the scalar metrics of equivalent sound level (L_{eq}), 8-hr equivalent sound level (L_{8eq}), L_{pk}, sound exposure level (SEL), kurtosis (Kurt), crest factor (CF), number of positive samples (Pos), number of negative samples (Neg), and duration (Dur). Power spectral density (PSD) was also computed. These metrics were examined for each type of noise source and Kurt and CF were found to be the only metrics which were good at discerning between impulse and non-impulse noises, since they are inherently good indicators of impulsivity. Two new metrics, spectral slope (m) and weighted-square error (WSE), were developed to capitalize on frequency domain differences between wind noise, impulse noise, and aircraft noise. Both metrics were based on the linear regression of a linear fit function for the PSD in the 2.5-100 Hz bandwidth. The metric, m, was determined from the PSD plotted on log-log axes. WSE measures the deviation of the PSD from a linear fit function, but is based upon PSD that has first been normalized. It was found that the two new metrics worked very well to complement the Kurt and CF time domain metrics. The final ANN structure achieved 100% accuracy on the training set of data and 99.6% accuracy on the evaluation set of data (but effectively considered 100% accurate, since the one false negative involved a distant blast (L_{pk}=92 dB) with high foreground noise).

Future work should address expanding the noise measurement library, determining the required hardware fidelity for the ANN approach, investigating alternate algorithms, creating a real-time implementation of the noise classifier in the laboratory, and a working prototype of the device for field-testing.

1.0 Objectives

The long-range goal of this 1-year exploratory effort was to create a noise monitoring system with higher accuracy at discerning between high-energy military impulse noise and other sources, while requiring no human intervention – in particular, develop a system that can automatically post results in a readily usable file format and disseminate results. Toward this goal, the development of the software for such an autonomous noise classification system was proposed, with the following specific aims:

- Create a library of noise recordings to include military impulse sounds and possible false positive sounds (wind, traffic, and possible wildlife interactions) to permit the off-line development of a new noise classifier.
- Investigate the possibilities of using ANNs with inputs of conventional acoustic metrics.
- If necessary, develop new metrics for use as inputs to the ANN based classifier

2.0 Background

2.1 Overview

Encroachment of civilian residences near military installations has become a significant problem in recent years. Civilian noise complaints and damage claims have forced military installations to reschedule, curtail, or even cancel training exercises that create high levels of military impulse noise (i.e. artillery, demolition training). It is well known that atmospheric conditions (e.g. wind, humidity, cloud cover, and temperature profiles) play a key role in propagation of noise, creating differences in the day-to-day noise levels experienced by surrounding communities. Contour maps of average predicted or measured noise levels in and around bases prove invaluable for predicting the impact of training exercises on surrounding communities, though they are not perfect. As such, some bases have employed noise monitoring systems around their perimeters in order to record the occurrences of high-energy military impulse noise events. L_{pk} and timestamp data are typically downloaded and post-processed daily and used to ascertain noise complaints and damage claims.

One popular system is the NoiseWatch® BLast Analysis and Monitor system (BLAM) developed by McQ [McQ]. It has been reported that the BLAM system suffers from an unacceptable degree of inaccuracy and further requires excessive human interaction. In particular, complaints include false triggers from wind or other noise (>10%) and poor detection of blasts below 115 dB, which is the current monitoring threshold for the system. Decreasing the threshold below 115 dB may exacerbate false wind triggers.

2.2 The BLAM Algorithm

The BLAM system algorithm is based on a sonic boom detection algorithm developed in the 1970s [Whiteford, 2005]. It works by analyzing both the amplitude and the shape of the signal. Although a geophone is included with the BLAM monitors, they are purportedly are not currently used in detecting blasts [Whiteford, 2005], owing to the differences in propagation speed through the air and ground, and the fact that the air wave can also excite the geophone. These issues are reportedly under further investigation.

The BLAM algorithm works quite well under idealized conditions; however actual conditions can be less than ideal. In particular, propagation effects, background noise, or multiple blasts can produce waveforms that confuse the algorithm. Some typical examples of such measured waveforms are shown in the top plots in Figures 1 and 2. Note that the spectrums (bottom plots in Figures 1 and 2) are relatively similar, despite the quite different waveform shapes (and test conditions). Wind gusts have also been reported to cause false positives from the BLAM algorithm, in particular at Fort Riley, KS, and Fort Carson, CO, [Whiteford, 2005; SERDP, 2003]. Despite these limitations, the BLAM is reported to generally work well for blasts with L_{pk}>119 dB, but less well when the L_{pk} is between 115-119 dB, and not at all for L_{pk} < 115 dB,

(the current design threshold). There is new interest in detecting blasts with much lower levels (as low as 100 dB) [Oles, 2005; Whiteford, 2005]. Although these lower levels would not be associated with causing damage or widespread disturbances, detecting them could at least corroborate noise complaints from the public, in order to validate complaints. Studies have indicated that merely expressing concern as part of public outreach program can lessen annoyance [Schomer, 1994]. Since the temporal characteristics of the blast waveforms can vary considerably, new algorithms for discerning military impulse noise from other sources are needed.
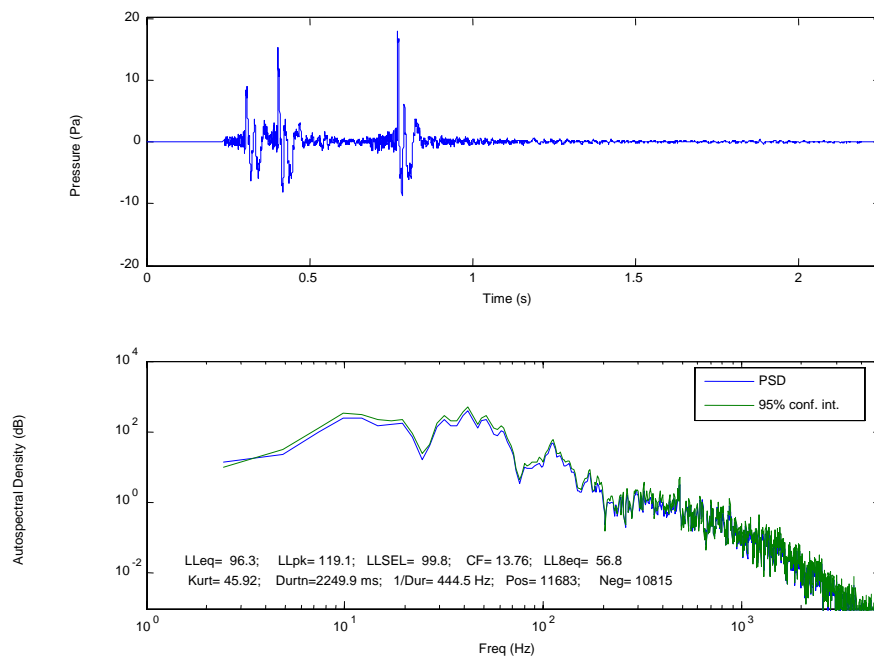

Figure 1. Three closely spaced 81mm mortar blasts measured at FITG, PA, 2000m from source with L_{pk}=119 dB. Top plot shows time history and bottom plot shows PSD.
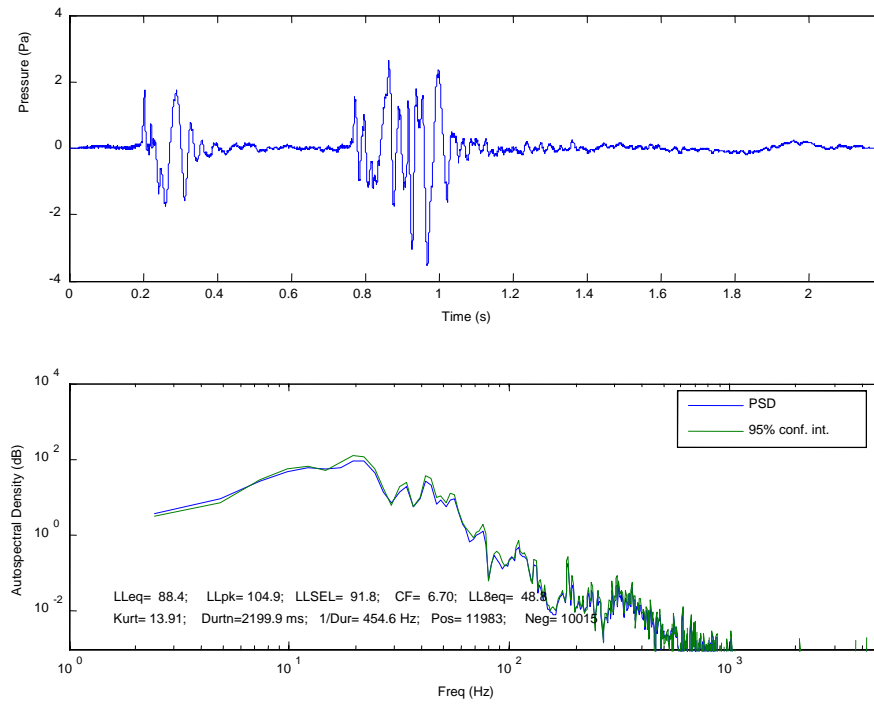
4

Figure 2. Two 81mm mortar blasts at MCBCL, NC, 3000m from source with L_{pk} = 115 dB. Top plot shows time history and bottom plot shows PSD.

3.0 Data Collection

3.1 Equipment

Since there was no off-the-self instrument or set of equipment that was suitable for collecting and recording very low-frequency impulse noise, various components were assembled into a custom system. This system was based upon a Larson Davis (LD) NMS-011 Environmental Noise Monitoring System (See Figure 3). The primary microphone was replaced with a Bruel & Kjaer (B&K) 4193 Infrasonic Microphone, which had a bandwidth of 70 mHz to 20 kHz. The primary microphone was connected via cable to a LD 824 Sound Level Meter (SLM). The LD 824 served as a field-portable microphone power supply that also logs L_{eq} and L_{pk} value at one second intervals (for subsequent data validation steps). Since most of the energy of the sources that were measured lies in the very low-frequency range (0-100 Hz) the weighting of the input spectrum was set to Flat (linear) Weighting; however post-processing can add any weighting desired. The LD 824 can also apply a gain to the output signal. This gain can be adjusted to improve the signal to noise (S/N) ratio in the measurements. The AC output of the LD 824 SLM was connected to a National Instruments (NI) DAQCard-6036E data acquisition card through a NI BNC-2110 input/output board. When weather permitted, a second channel was recorded using a LD 2540 microphone with a B&K 5935 power supply. The DAQCard was installed into a Dell Latitude laptop with a Pentium IV processor. A Virtual Instrument (VI) was created in Labview 7.1 to capture waveform data. The VI enabled an "automatic

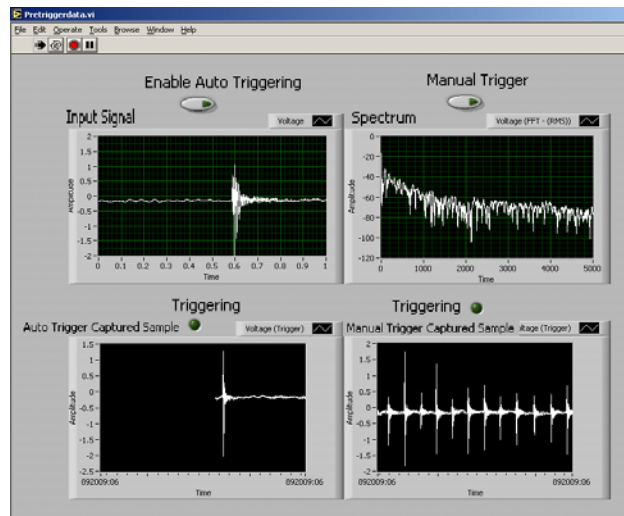Figure 3. Noise recording equipment in the field.

Figure 4. Screen Shot of VI

triggering/pre-triggering mode," where data were recorded when the signal exceeded a specified threshold, (used to automatically record impulse events – this corresponds to exceeding a certain L_{pk} value). Although the threshold can be set to record at or above any desired L_{pk} level, it was typically adjusted to just above ambient noise levels in order to record as much data as possible. In our data collection, a 0.1-0.25 second pre-trigger was coupled with an additional 2 seconds of recorded data for each record. By pre-triggering, the entire event was able to be recorded. A manual (continuous) triggering mode was also possible, which was used to record longer or continuous events such as wind, aircraft noise, traffic, and engine noise. During multiple successive trigger events, the "automatic mode" also triggered nearly continuously. A screen shot of the VI is shown in Figure 4. The VI displays the current instantaneous time signal (upper left Fig. 4), the instantaneous spectrum of the input signal (upper right Fig. 4), a captured waveform obtained with the automatic triggering mode (lower left Fig. 4) and multiple waveforms captured using the manual triggering mode (lower right Fig. 4). The VI also contained buttons to toggle between the different modes of operation. Although most of the military impulse noise energy was in the very low frequency range (0-100 Hz), to provide maximum flexibility in the algorithm development, data were sampled at 10 kHz.

3.2 Data Collection Procedure

Military impulse noise and wind noise data were collected at MCBCL, NC, and FTIG, PA (two different trips). Wind data were recorded in central Ohio and suburban Pittsburgh. Additional wind data were recorded at MCBCL and FTIG.

Before conducting trips to the military installations, range control officers were consulted to determine the best times to visit the installations (based upon extensive training exercises with a variety of noise sources). The range control personnel were able to point out areas where high levels of noise and/or a high frequency of noise complaints would occur. At MCBCL, measurements were conducted in the vicinity of the most active permanent NoiseWatch® BLAM stations, in order to get accurate representations of the signal that the monitors try to classify. Upon arrival at a selected location a setup procedure and checklist was conducted in order to prepare the equipment for data collection. At this point the location, barometric pressure, date, time, wind speed (if applicable), and weather conditions were recorded in the test log. During the data collection, a time and event history was also recorded in the test log in order to verify each noise source during subsequent post processing of the data. Changes in weather conditions were also periodically noted.

During the trips to central Ohio and suburban Pittsburgh for recording of wind noise, locations were selected to maximize wind velocity while minimizing background noise. These locations were at the highest possible altitude, free of surrounding structures and trees and absent of other types of background noise. The instrument setup was identical to that used for the measurements taken at the military installations, however manual (continuous) triggering was typically used.
In all, 1000 usable wave forms have been collected, including 330 military impulse events and 670 non-impulse events. Military impulse noise data included 155mm Howitzers, 81mm mortars, 60mm mortars, 60mm rockets, 40mm grenade launchers, A-10 30mm cannon strafe, M67 hand

grenades, and Bangalore Torpedoes (strings of 3, (27lbs HE)). Regrettably, despite meticulous care and real-time signal monitoring, some of the data were corrupt due to cabling problems, and had to be discarded. Therefore, some of the sources above are not represented (M67 hand grenade and 60 mm mortars). Different measurement locations included the edge of bodies of water, flat open fields, flat wood lands, tops and bottoms of ridge lines, and thick, mountainous woodlands. Since most of the data were collected during the late spring and summer, temperatures ranged from around 75 to 100°F. Relative humidity levels varied from 44% to 100% (raining). Non-impulse (potential false positive) data included winds, aircraft (F-16, A-10, and C-130), traffic, and woodland noise. Although by no means exhaustive, the current library is deemed adequate for the preliminary development and evaluation of the real-time noise classifier algorithms. The library of records is being supplied on compact discs (CD), as it is hoped that they will be useful for future military studies. All system gains and calibration constants have been applied so that the signals have units of Pascals. Data were stored in ASCII format.

4.0 Data Processing

4.1 Conventional Metric Processing

As was originally proposed, the data were processed to extract the acoustic metrics of L_{eq}, L_{8eq}, L_{pk}, SEL, Kurt, CF, Pos, Neg, and Dur. Kurt is defined as the fourth central moment divided by the standard deviation to the fourth power (typically used as a measure of how "outlier-prone" data are):

$$Kurt = \frac{E[p^4]}{\sigma^4} = \frac{1}{\sigma^4 T} \int_0^T p^4 dt. \qquad (1)$$

T is the length of time over which Kurt is computed (in our case, the length of the recording) and σ is the standard deviation of the sampled acoustic pressure, p. CF is computed as

$$CF = \frac{\max(p)}{p_{rms}}. \qquad (2)$$

L_{eq} is the equivalent sound level over the recording period (approx. 2 seconds). The Enhanced Sound Level Meter (ESLM) code developed at the University of Pittsburgh was used to compute these metrics along with the PSD of each waveform (N_{FFT} = 4096 points, overlap=50%, window=Hanning). Figure 5 shows the output of an example waveform processed by the ESLM code, where the upper plot displays the captured time history and the bottom plot depicts the PSD of the waveform. The scalar metrics for this particular event are displayed below the plots, just above the caption. These values were also exported to text files, which in turn served as the input to the ANN algorithm. The computed metrics for all of the collected waveforms have been supplied in the Excel file: ESLM_Signal_Metric_Outputs.xls, which is provided on the DVD as well as an attachment to this report (see Appendix A).
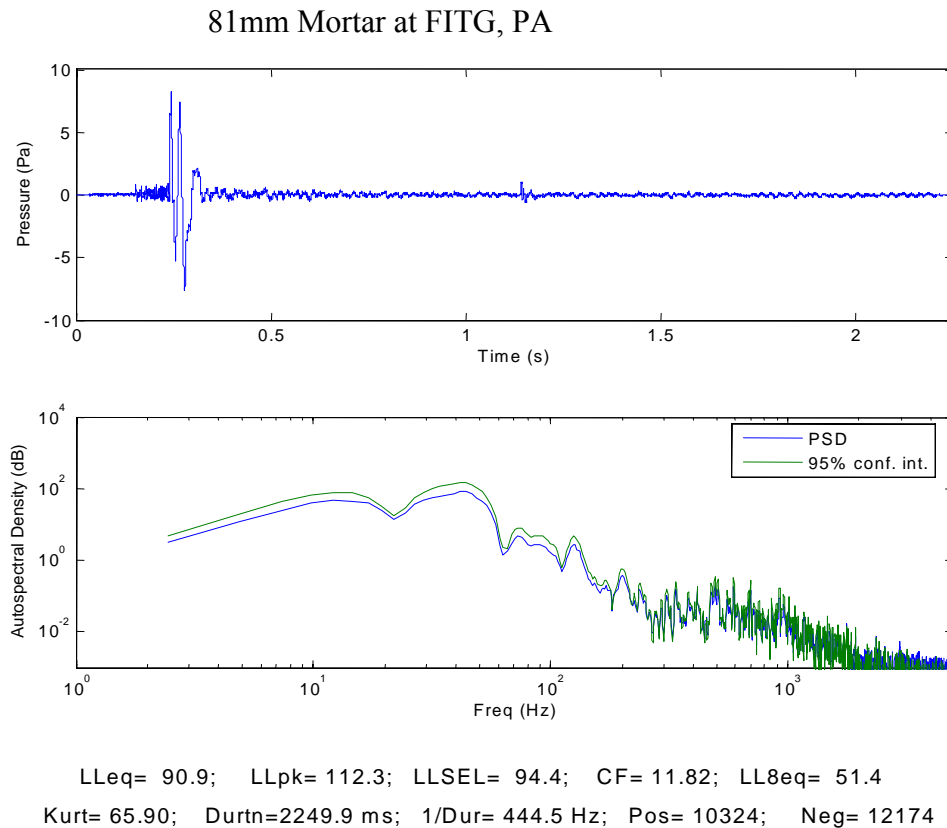
81mm Mortar at FITG, PA

LLeq= 90.9;   LLpk= 112.3;   LLSEL= 94.4;   CF= 11.82;   LL8eq= 51.4

Kurt= 65.90;   Durtn=2249.9 ms;   1/Dur= 444.5 Hz;   Pos= 10324;   Neg= 12174

Figure 5. Typical 81mm Mortar blast measured at FITG, PA at a distance of 2 km (L_{pk} = 110 dB).

Once all the waveforms had been processed, the results were analyzed to see if particular metrics appear to be better at discriminating between military and other sources of noise. A plot of the more useful metrics (ordinate) for the 1000 collected waveforms (abscissa) is given in Figure 6. The first 670 points represent recordings of nonmilitary impulse noise and the remaining 330 points represent military impulse events. When comparing the two groups of data, the metrics were found to be similar, with the exception of Kurt and CF. These two metrics have been used in the past for characterizing impulsive type sounds [Henderson, 1986; Hamernick, et al., 1993; Vipperman, et al., 2003]. It was expected that these two metrics would be the most useful for noise classification.
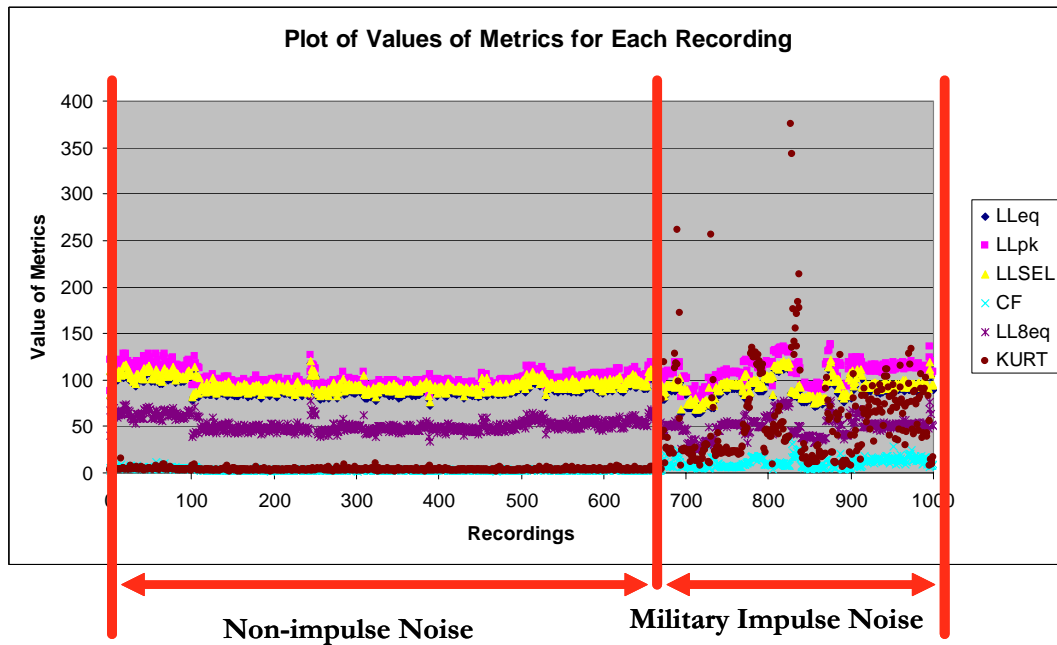
Figure 6. Plot of Acoustic Metrics for each Waveform

4.2 Preliminary ANN

An ANN is an interconnected assembly of simple processing elements called units or nodes, whose functionality is loosely based on the animal brain [Kosko, 1992]. The processing ability of the network is stored in the inter-unit connection strengths, or weights, obtained by a process of adaptation to, or learning from, a set of training patterns. Multiple ANN structures were examined, the first of which is shown in Figure 7. This network simply takes all of the scalar signal metrics computed by the ESLM code as inputs and tries to determine whether the waveform was military impulse noise or not (single binary output). The hidden layer adds complexity to the network, which typically improves performance. The use of multiple hidden layers of various sizes was investigated, but no improvement was gained. As is typical, the ANN complexity was usually increased until no further benefit was derived. The ANN was trained using the Levenberg-Marquardt algorithm [Kermani 2005].
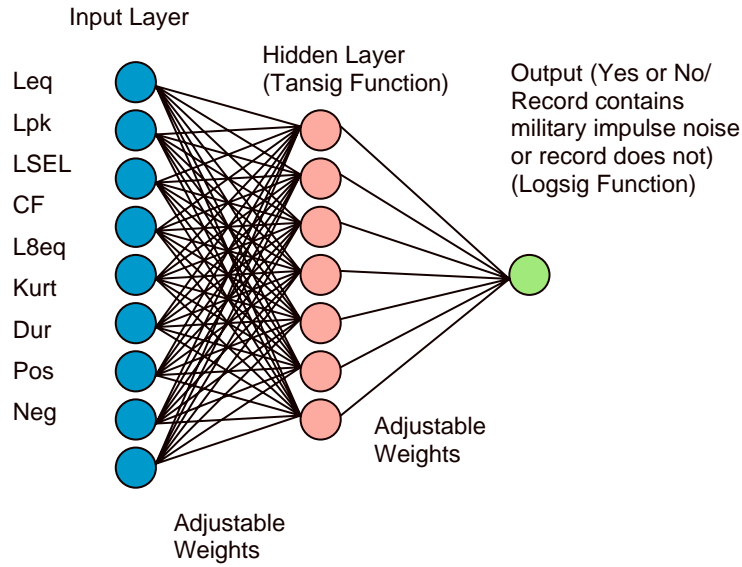
11

Figure 7. Topology of First ANN Structure.

The data were randomly divided into two parts: 2/3 were used for training purposes and the remaining 1/3 was used for evaluation. Initially, the data recorded at MCBCL were used, since no other data were available at the time. An accuracy of 96% was achieved during the validation phase. When new data were subsequently collected from FTIG and used to validate the classifier, an accuracy of only 92% was achieved (with no new training – some improvements would be expected if the network were also trained on the FTIG data, which had different characteristics due to the topological differences).

The results indicated that the ANN-based algorithm had potential to distinguish between military impulse noise from other noise sources, although there was still sufficient room for improvement in the algorithm. Specifically, improvements in accuracy were sought by decreasing the dependence upon the temporal shape of the waveform as well as the overall magnitude (L_{pk} value). The next section will describe new metrics that were developed to achieve these goals.

4.3 New Scalar Metrics for Use as ANN Inputs

Analyzing the PSD of a waveform was an attractive option, since the factors such as location, weather, terrain, number of events, multi-path propagation and timing of the events can strongly affect the temporal characteristics of a waveform. When comparing PSDs of the many different waveforms of military impulse and non-impulse noise records, some commonalities become apparent. First, most of the energy of the signals that have been analyzed usually lies within the 0-100 Hz bandwidth (as expected). Also the shapes of PSD curves between 0-100 Hz, for similar sources, usually had similar features. The three main noise types to be considered here were wind noise, military impulse noise, and aircraft noise.

Figure 8 shows a typical PSD plot for a wind noise record. A classic von Karmon–type spectrum [Blevins, 2001] was observed. That is, when wind PSD was plotted on log-log axes, the energy was predominately low frequency and has a linearly decreasing trend. An increase or decrease of velocity will shift the PSD curve to the right or left, respectively, with little change to the actual trend. Note that a linear regression with a linear fit function performed on the PSD between 2-100 Hz would be expected to have relatively little error.
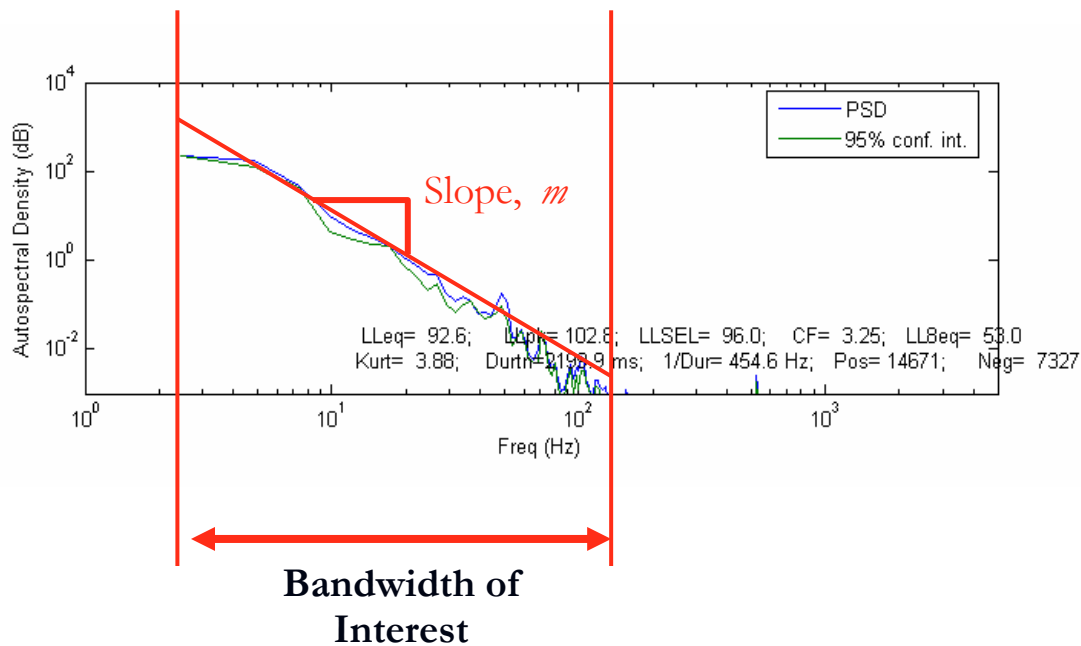
Figure 8. Typical PSD plot of wind noise

Figures 9 through 11 shows some typical PSD plots of military impulse noise sources (81mm mortar, Bangalore torpedo, and 155mm Howitzer, respectively). When comparing these figures, within the bandwidth of interest, it becomes apparent that these curves were very different in structure from the wind PSD, yet have features in common with themselves. For example, each of the curves begin with an increasing slope (up to 10-20 Hz), become level (between 10-50 Hz), and transition to a negative slope (20-100 Hz). These curves were not well represented by a linear trend, as with the wind noise.
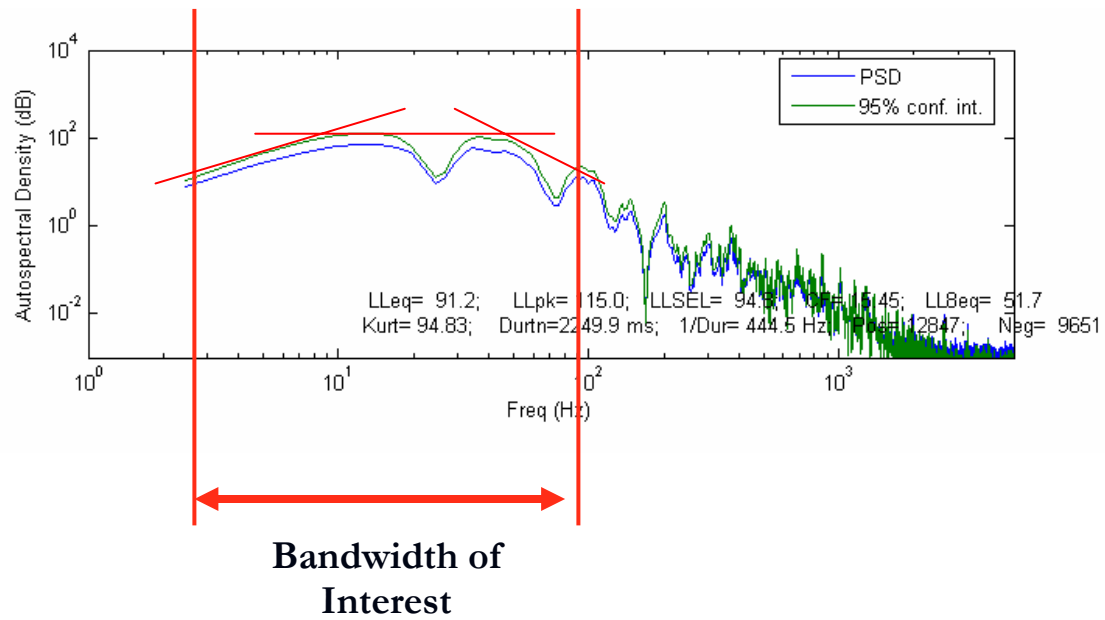
Figure 9. Typical Plot of PSD of 81mm Mortar
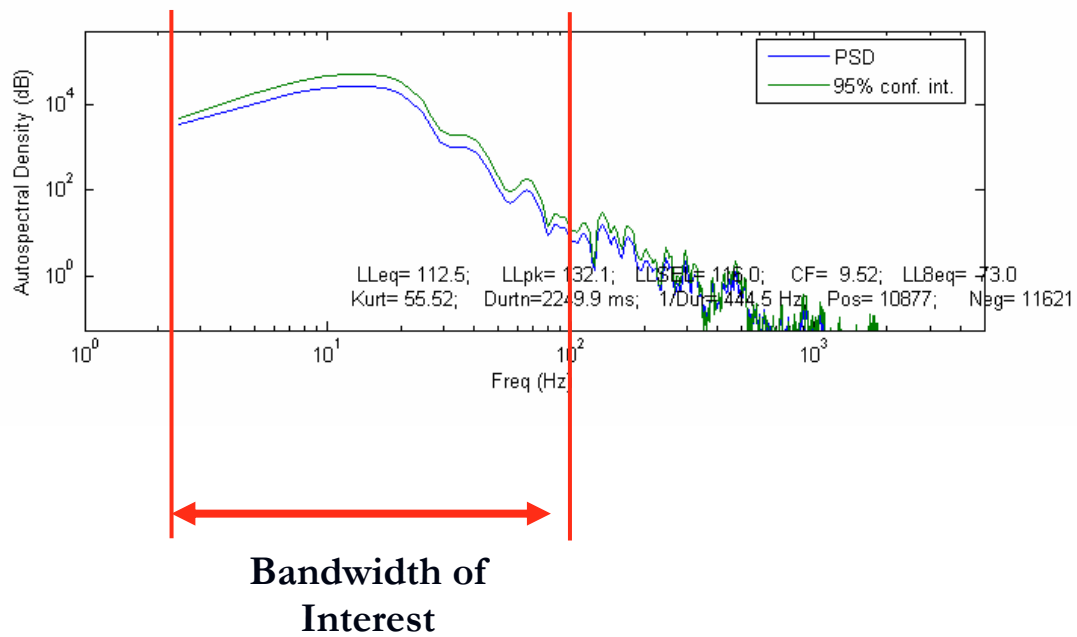
Figure 10. Typical Plot of PSD of Bangalore Torpedo

Bandwidth of Interest
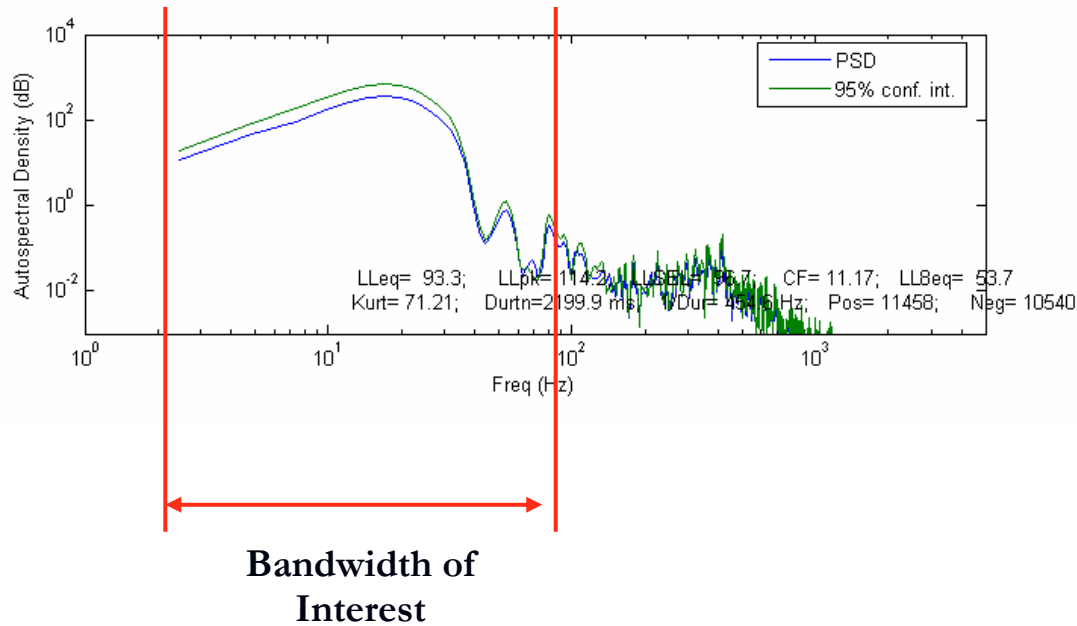
Figure 11. Typical Plot of PSD of 155mm Howitzer

The PSD plot of typical aircraft noise is shown in Figure 12, where it is seen that the signal energy often has a much wider bandwidth (0-2,000 Hz) than the impulse noise. The overall slope of the PSD curve within the bandwidth of interest (0-100 Hz) was closer to "flat" (zero slope) than that of military impulse noise or wind noise.

Bandwidth of Interest

Figure 12. Typical Plot of PSD of F-16 Flying Over

With these commonalities identified, it now became possible to develop frequency-domain metrics that encompassed these generalizations.

4.4 Development of New Metrics for Input to ANN Structure

Two new metrics were created to take advantage of the observed differences in PSDs – the m and the WSE. Both metrics were scalar and apply to the 2.5-100 Hz bandwidth of the PSD. Scalars were desirable as inputs to the ANN, since they keep the complexity down. The metrics have 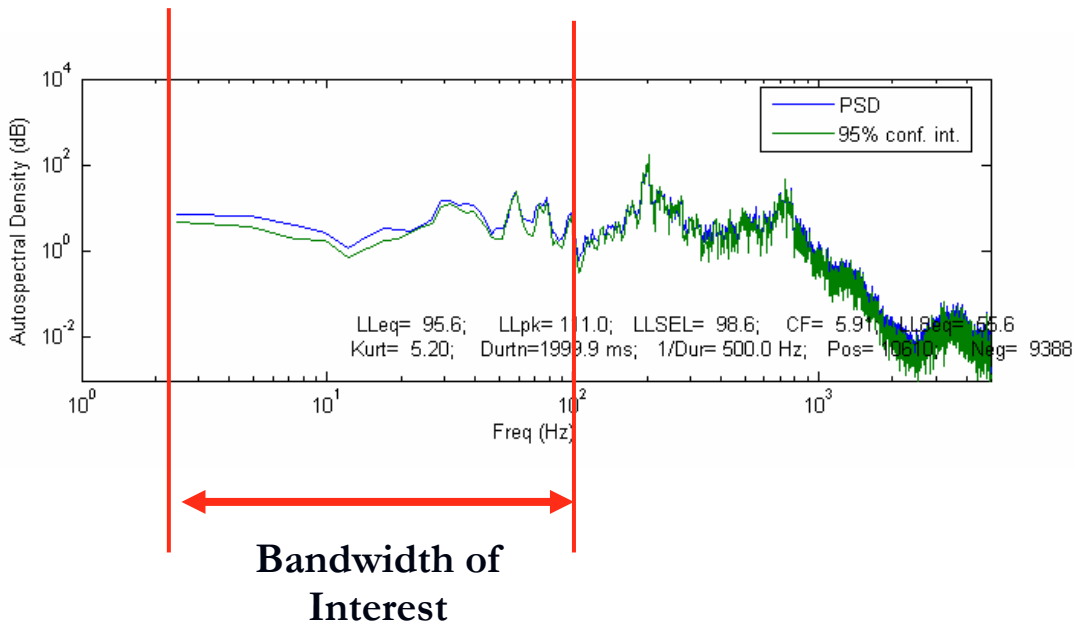been combined with Kurt and CF, which were described in section 4.1, and found to be good indicators of the impulsiveness of the noise. Although they were time-domain algorithms, they were inherently not as strongly dependent upon detecting a waveform with a particular shape, as with the BLAM algorithm.

4.4.1 m

m was computed by creating a least-squares fit to a line, $\hat{y} = mx + b$, where $\hat{y} = \log_{10}(PSD)$ was the base-10 logarithm of the PSD and $x = \log_{10}(f)$ is the base-10 logarithm of frequency. The fit was conducted over the frequency bins between 2.5 and 100 Hz. Although the impulse noise sources were poorly characterized by a linear trend, the slope was still useful for differentiating from other types of noise, as will be illustrated later.

4.4.2 WSE

The "goodness" of the fit was assessed with the WSE, which was computed as

$$WSE = \sum_{i=1}^{41} [y_i - \hat{y}_i]^2 [f_{i+1} - f_i]. \tag{3}$$

where y_i was based upon the $\log_{10}(PSD_i)$ of the ith frequency bin, which was given by equation (4) (below), $\hat{y}_i$ was the estimate of y_i from the linear curve fit, and f_i was the ith frequency. Squaring the quantity $[y_i - \hat{y}_i]$ allowed WSE to remain positive to reflect the total magnitude of the error. The term $[f_{i+1} - f_i]$ served to add greater weight to the difference between y from $\hat{y}$ at the lower frequency bins. This was done because the best features for identifying military impulse noise from non-impulse noise occur at the lower reaches of the bandwidth of interest. There were 42 frequency bins from 2.5-100Hz for the given spectral resolution, and the WSE was computed from the first 41 of these bins. In order to scale the metrics with respect to signal energy, the logarithmic PSD terms, y_i, were normalized to have a value between 0 and 1, which correspond to the minimum and maximum values of $\log_{10}(PSD)$, respectively. Thus, y_i was computed as

$$y_i = \frac{\log_{10}(PSD_i) - \min(\log_{10}(PSD))}{\max(\log_{10}(PSD)) - \min(\log_{10}(PSD))} \tag{4}$$

4.5 Explanation of New Metrics

The next set of figures will illustrate the utility of the WSE and slope metrics in classifying the encountered types of noise sources. When they were applied to wind noise, as in the case of the record presented in Figure 8, the resulting slope is $m = -4.29$ and WSE = 0.0093. Figure 13 shows normalized data and curve-fit results in the region of interest, where the *x*-axis represents $\log_{10}$ (frequency (Hz)) across the 2.5–100 Hz band. The WSE of 0.0093 was relatively small because the linear approximation was quite good for wind noise. It is important to note that the green slope line shown in Figure 13 is not exactly the same thing represented by the slope metric, *m*, described above. While Figure 13 shows the slope of the *normalized* PSD function, *m* was actually computed using the *non-normalized* values of PSD. Both slopes were examined, but the one chosen provided much better signal detection abilities. For the blast represented in Figure 13, the corresponding non-normalized slope was $m = -4.29$. The negative value for *m* was a result of the roll-off in spectral energy with increasing frequency.

Figure 13. Plot of normalized $\log_{10}$(PSD) and linear curve fit versus $\log_{10}$(frequency) for wind noise (2.5-100 Hz) given in Figure 9.

Next, the frequency-domain metrics were applied to military impulse noise event presented in Figure 9. For this case, $m = -3.36$ and WSE = 0.679, with the graphical comparison between the data and curve fit given in Figure 14. The slope was somewhat similar to that for the wind noise (25% smaller), however, the WSE was more than 70 times larger than the wind noise, as a result of the poor linear fit for the data.
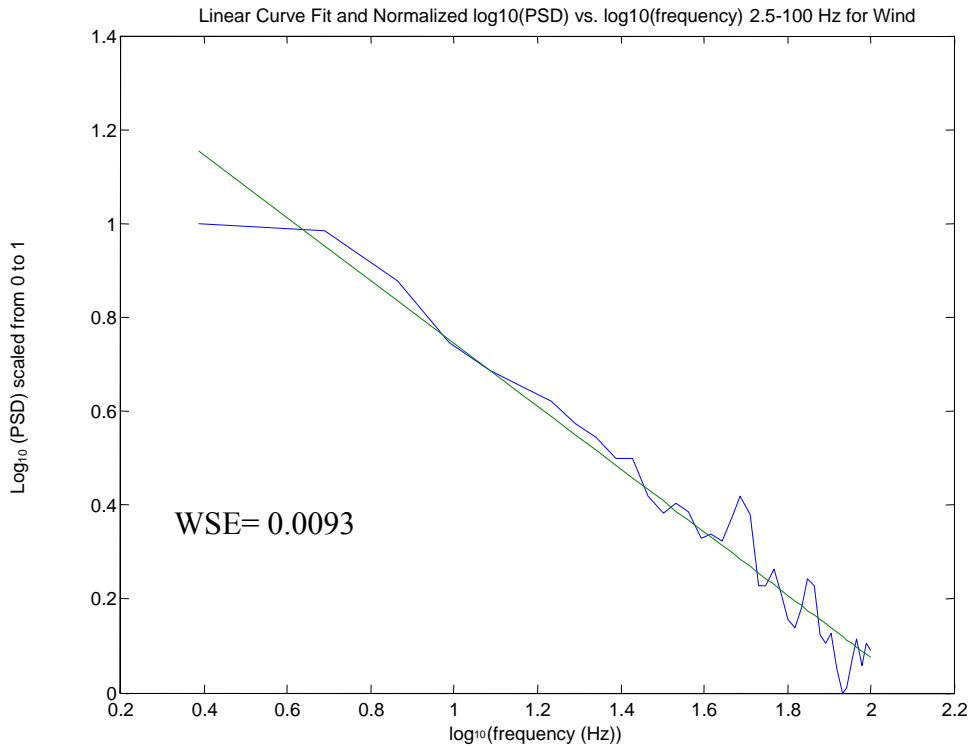
17
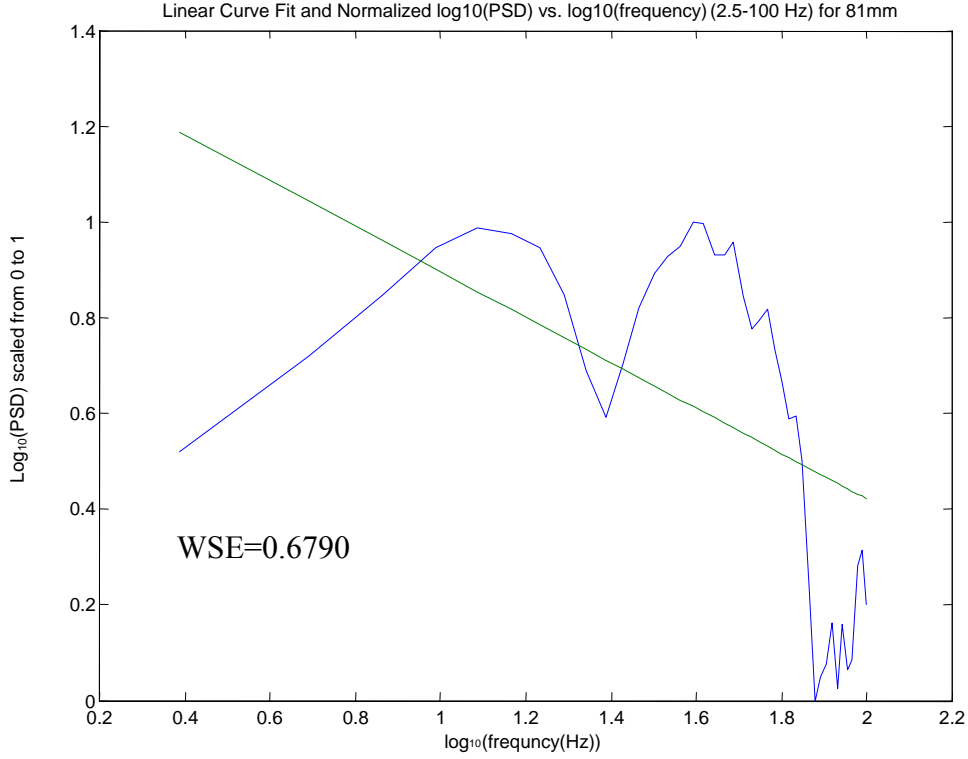
Figure 14. Plot of normalized $\log_{10}$(PSD) and linear curve fit versus $\log_{10}$(frequency) for an 81mm Mortar (2.5-100 Hz) given in Figure 10.

Figure 15 shows the results for the aircraft noise record presented in Figure 12 (m = 0.326 and WSE =0.0642). In contrast to the other sources, the slope of the curve was slightly positive and considerably smaller (factor of 10). Whether the slope was positive or negative, it was typically small (relatively flat frequency response) for this type of noise. The WSE was larger (by a factor of 7) than the wind noise but considerably smaller than the impulse noise (by a factor of 10). These results, which were summarized in Table 1, illustrate that the different noise sources produce distinguishable differences in the new frequency-domain metrics. Table 2 summarizes the qualitative results of using m and WSE for noise classification. The new scalar metrics were very amenable to being included as inputs to the ANN noise classifier.

Table 1. Output of New Scalar Metrics

| Main Types of Noise Sources	Value of m	Value of WSE
Military Impulse	-3.36	0.679
Wind	-4.29	0.0093
Aircraft	0.326	0.0642
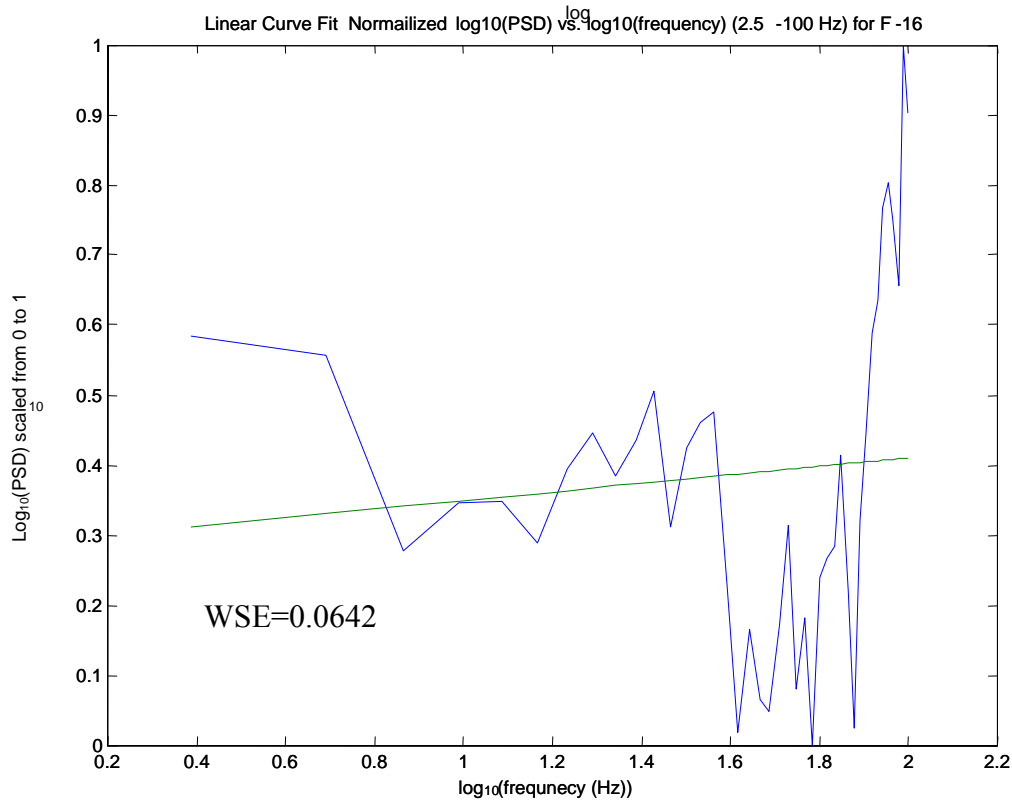
Figure 15. Plot of normalized $\log_{10}$(PSD) and linear curve fit versus $\log_{10}$(frequency) for an F-16 flyover (2.5-100 Hz) given in Figure 13.

Table 2. Summary of the Expected Output of New Scalar Metrics

Main Types of Noise Sources	Relative Value of m	Relative Value of WSE
Military Impulse	Large Negative	Large
Wind	Large Negative	Small
Aircraft	Small Negative or Positive	Moderate

Figure 16 shows the values for m (bottom plot) and WSE (top plot) for each of the recorded waveforms, similar to Figure 6 for the ESLM code outputs. The non-impulse data given in Figure 16 are further divided into aircraft noise ("Section A") and wind noise ("Section B"). It was apparent that the data presented in Figure 16 agrees well with the observations given in Table 2, although there were a few outliers. The most noticeable of these would be the positive values for m in a few of the military impulse noise records. These waveforms corresponded to relatively quick events, closer to the definition of a true impulse, such as 81mm mortar launches, grenades, and 60mm rockets breaking the sound barrier or blasts occurring in close proximity. An example of such a set of events is shown in Figure 17. Fortunately, these fast peaking events have comparatively large values for Kurt and CF because they peak and end quite rapidly. The ANN structure was able to take into account the high values for Kurt and CF and thus produce a correct noise classification. Some outlying points also occurred in the non-impulse noise records. These events were often wind or aircraft noise with comparatively low L_{pk} values. Once again, the Kurt and CF values were able to correctly classify the noise the wind noise. By the same token, m and WSE values complement the Kurt and CF at times. Such a case can occur when multiple impulse events happen in a very short period of time, different events occur simultaneously, or events were not extremely loud causing Kurt (Equation 1) and CF (Equation 2) to be relatively smaller in size. However, the PSD of multiple impulse events was very similar to single events, meaning that the m and WSE will be relatively unaffected. Figure 18 shows the waveform and PSD resulting from three very distant 155mm Howitzer blasts that overlay one another. In this case the metrics, Kurt and CF yield an inconclusive result but, m and WSE can identify the events as military impulse noise. Thus, the two sets of metrics were shown to compliment one another, and improve the overall accuracy of the impulse noise identification system.
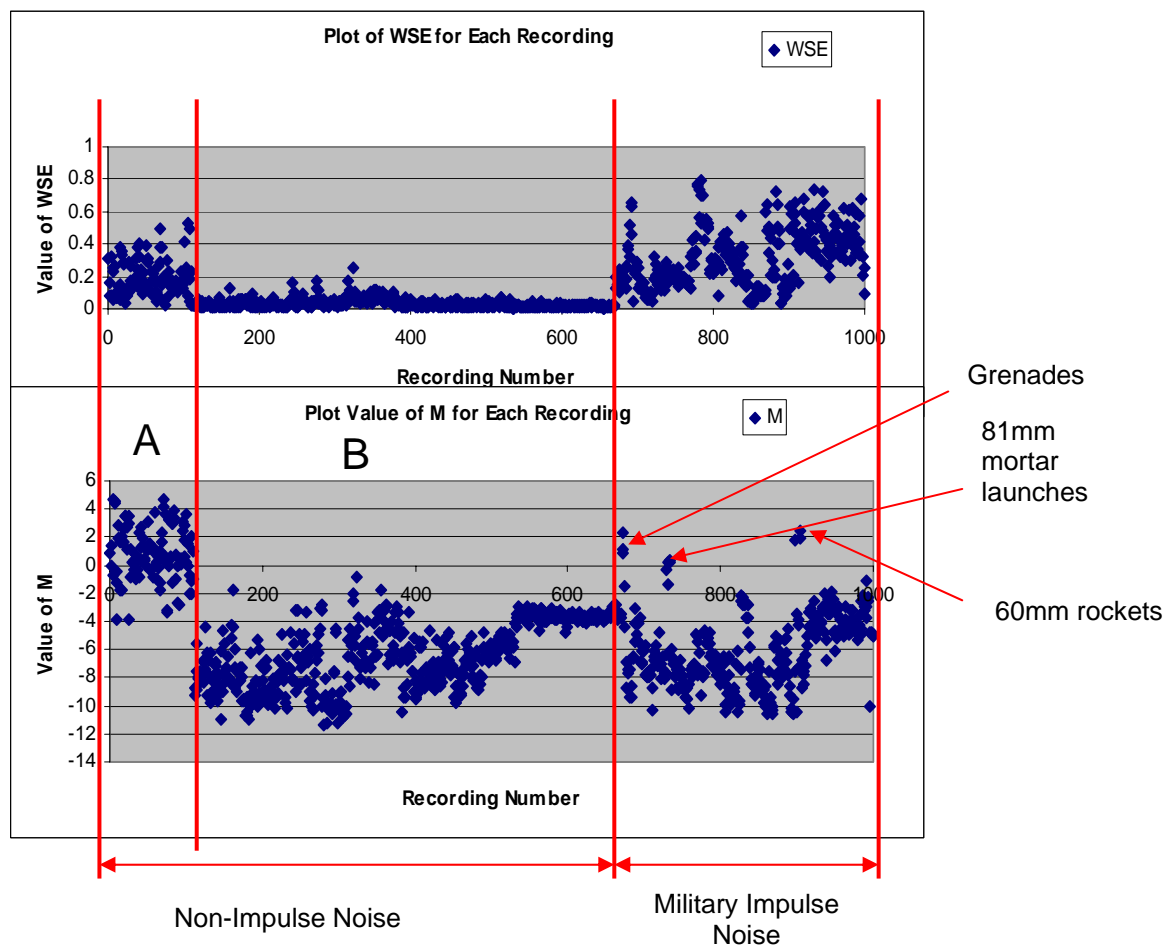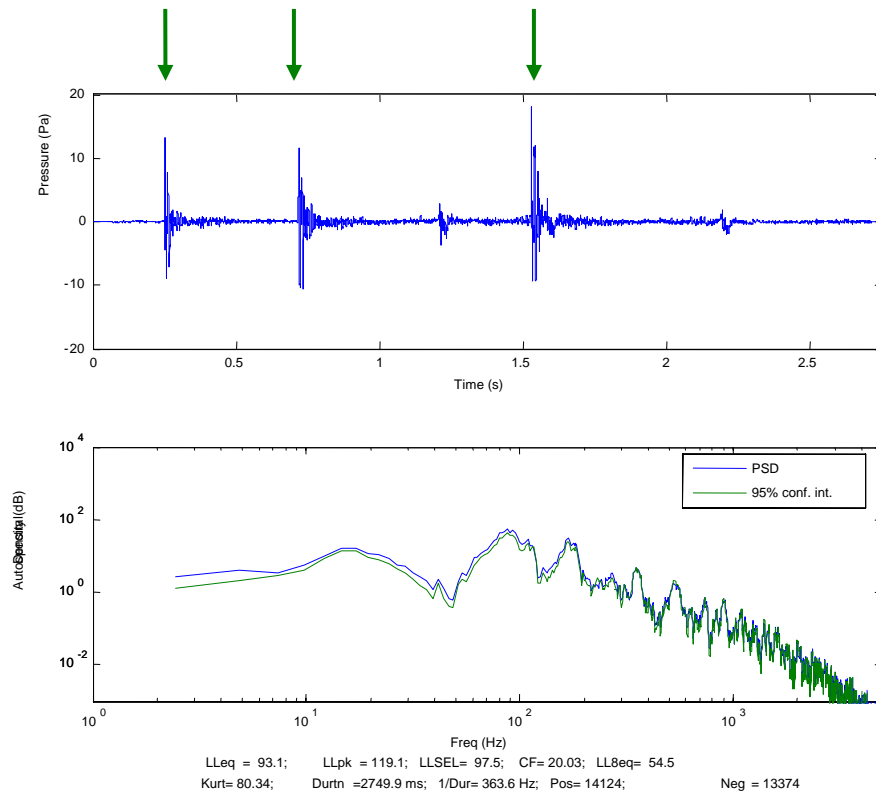
Figure 16. Values of *m* and WSE for each Waveform

Figure 17. Three (denoted by green arrows) 60mm Rockets fired from A-10 at 2000m at FTIG, PA: *m* = 2.49, *WSE* =0.155, Kurt =80.3, CF=20.0, L$_{pk}$=120 dB.

LLeq = 80.3;   LLpk = 93.0;   LLSEL= 83.9;   CF= 4.31;   LL8eq=
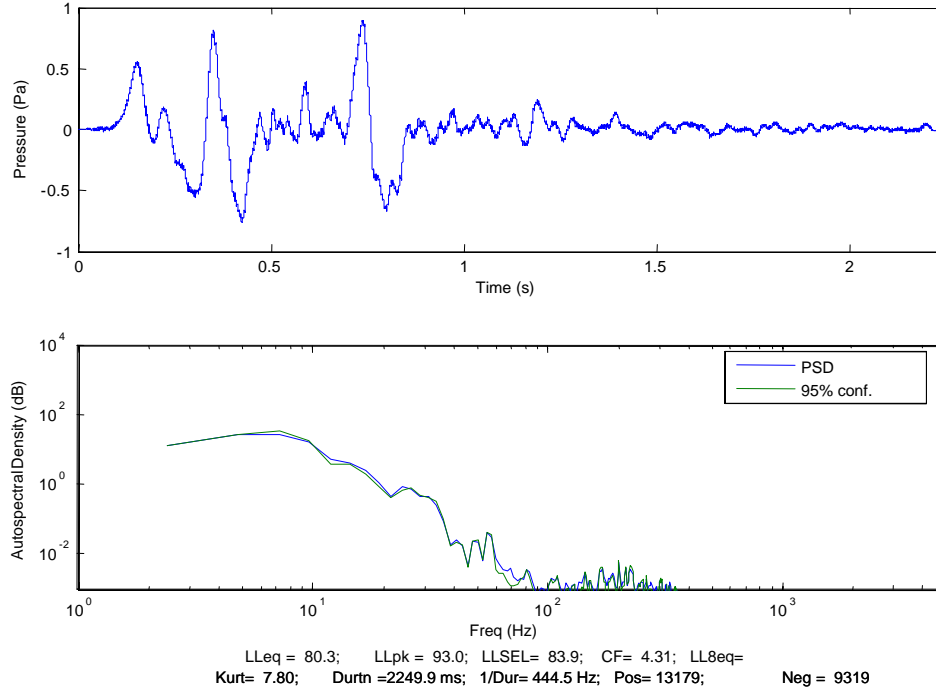Kurt= 7.80;   Durtn =2249.9 ms;   1/Dur= 444.5 Hz;   Pos= 13179;   Neg = 9319

Figure 18. Three overlayed 155mm Howitzers recorded at from 6 to 10 km at FTIG, PA.
$m = -10.5$, $WSE = 0.124$, Kurt=7.80, CF=4.31, L_{pk}=93dB

4.6 Revised ANN Structure

Multiple structures for the ANN classifier were investigated, but the final topology was given in Figure 19. The four inputs were WSE, m, Kurt, and CF. The temporal metrics of Kurt and CF were retained in the design because they offer the best indication of the impulsiveness of a signal. Three hidden layers of 4-nodes each (tan-sig squashing functions) provided the best performance while minimizing complexity.   This ANN structure was also trained using the Levenberg-Marquardt algorithm [Kermani 2005]. The ANN achieved an accuracy of 100% on the training data and 99.6% accuracy on the test data (one incorrectly classified waveform out of 287). The single incorrectly classified record was a false negative. It should be pointed out that when this case was examined closely, it was determined that the waveform had an L_{pk} of only 92 dB (so distant, that it is likely not of interest) and the waveform was measured with a HMMWV idling in the foreground. For practical purposes, the results are considered 100% accurate.
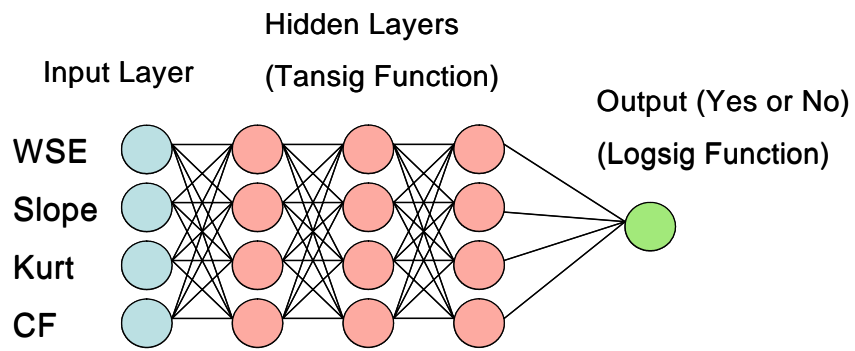
23

Figure 19. Topology of Second ANN Structure

5.0 Conclusions

This report summarizes an effort to develop a more accurate autonomous noise classifier. Current monitoring systems have been reported to suffer from false positives and numerous unidentified events, as well as limited ability to detect military impulse events with L_{pk} below 115 dB. The specific aims of this project were to: collect a library of military impulse noise and signals that were known sources of potential false positives as well as to develop an ANN and associated algorithms necessary to classify sources as military impulse noise or not. Approximately 1000 usable waveforms of various sources have been collected from MCBCL, NC, FITG, PA, Central Ohio (wind only), and Pittsburgh, PA (wind only). Useful military impulse noise recordings include 60mm rockets, 81mm mortars (firing and impact), 155mm Howitzer (firing and impact), 30mm Gatling gun strafe (GAU-8), 40mm grenades, and Bangalore Torpedoes. Non impulse noise sources included wind, operational noise, and aircraft (e.g. close air support during training). The algorithm development involved an ANN training phase followed by an evaluation phase. New scalar metrics, *m* and WSE, have been developed to be used as inputs to the ANN. Both metrics were dependent upon a linear curve fit of the normalized, low-frequency (<100 Hz) PSD function. Two other time-domain metrics, Kurt and CF, serve as inputs to the ANN noise classifier, since they were excellent metrics for the "impulsiveness" of a signal. All four metrics were less dependent upon a particular shape of the blast waveform, unlike the BLAM algorithm. A single binary output from the ANN indicated whether a particular event is military impulse noise or not. The final ANN structure was found to produce an accuracy of 99.6% (but effectively considered 100% accurate, since the one false negative involved a distant blast (L_{pk}=92 dB) with high foreground noise). All algorithms were developed in MATLAB and were amenable to a real-time implementation.

6.0 Future Work

The results of this exploratory effort were very encouraging. It should be pointed out that although time signals were recorded and used for the development of the algorithms, they are not required for the operation of a permanent version of the monitoring system. That is, a real time implementation can be created. Interest has been expressed by USA-CHPPM and MCBCL to implement the new algorithms on the existing NoiseWatch® BLAM [McQ] hardware. Toward this goal, some recommendations for future work include:

1. Make additional noise measurements in the field to create more exhaustive noise library
2. Retrain the ANN classifier, incorporating the above new data
3. Investigate alternate and possibly more robust algorithms, such as Bayesian learning approaches
4. Streamline the best algorithms for computational efficiency
5. Create and test a real-time implementation of the noise classifier in the laboratory
6. Determine the required hardware fidelity for the algorithms to work well
7. Assess the BLAM hardware and determine whether upgrades are necessary
8. Port the algorithms to the BLAM hardware or other field-trial hardware
9. Perform field testing of prototype at selected military base(s)
10. Full implementation of the technology (with McQ)

Although the classifier could be trained using data specific to each base, it is more desirable to have a generic solution that will work for any military base. To ensure the generality of the algorithms, additional data should be obtained from other locations, in particular, other topographies (e.g. the plains of the Midwest) and weather conditions (e.g. snowing/snow cover). Wind measurements at Forts Riley and Carson are also advisable, since these are the locations noted by USA-CHPPM as having excessive wind triggers. If detection of sonic booms is also desired, they should also be measured, along with any other known sources of false positives (one installation reported that birds pecking at deteriorated, insect-infected windscreens have created triggers). These data can then be combined with the current data set and used to retrain and evaluate the ANN structure. In the event that accuracy is found to suffer with the new data, adjustments to the ANN structure can likely be made to address that issue.

At the same time, probabilistic learning algorithms [McKay, 1992] should be studied that might provide better robustness, particularly across military installations. In particular, Bayesian methods have proven effective in many applications of parameter estimation and spectral analysis [Bretthorst, 2001; Sivia, 2006] and have successfully been applied to filtering processes, such as discerning between legitimate and "spam" email messages with reported accuracies as high as 99.5% [Graham, 2003]. These target applications have goals that are similar to the noise classification problem.

The signal metrics computed for the ANN classifier are currently based upon the ESLM code developed at the University of Pittsburgh, which emulates a digital SLM in accordance with ANSI standards S1.4, S1.11, and S1.43, including the detector circuitry (impulse, fast, or slow time constants), the weighting networks, and integrated metrics, such as L_{eq}. The code is

implemented in both the time and frequency domains, in accordance to whichever is most efficient. Not all of the functionality of the ESLM code is necessary for a real-time classifier implementation. The ESLM code is also not necessarily computationally optimized for this specific application, but could be. For example, most digital signal processor (DSP) chips have special memory addressing modes to make computing fast Fourier transforms (FFTs) and implementing digital finite impulse response (FIR) or infinite impulse response (IIR) filters very quick. A real-time implementation should take advantage of these modes for efficiency. Other techniques, such as zoom FFT processing, can also be utilized to improve computation time.

The algorithms should first be ported from MATLAB to a DSP chip in the laboratory environment. The recorded waveforms can be "fed" to the real-time implementation as if they were just sampled in order to test the code and ensure that the behavior is identical to the off-line version developed in MATLAB. This will also permit the algorithm to be streamlined to the extent possible. Once this is complete, the algorithms can be ported to the NoiseWatch® BLAM [McQ] or other desired hardware (somewhat chip-specific), providing the equipment meets the requirements of the algorithm. In particular, the bandwidth and dynamic range requirements for the new algorithm must be established in order to determine whether the NoiseWatch® BLAM [McQ] hardware should be upgraded. Every effort will be made to utilize the existing hardware. However, given rapid advances in technology, upgrading to a faster and less power-intensive DSP chip may be an attractive option.

Finally, it may be possible to expand the classification of the system from the simple "yes/no" categorization of detecting impulse noise or not to actually recognizing different weapon systems. This may be of interest to the military for recognizing friend or foe fire, for example and assessing complex situations in warfare, in particular urban warfare conditions.

7.0 References

Cited Literature

ANSI S1.4-1983 (R2001). 2001. Specification for Sound Level Meters, American National Standards Institute, New York, NY.

ANSI S1.11-2004. 2004. Specification for Octave-Band and Fractional-Octave-Band Analog and Digital Filters, American National Standards Institute, New York, NY.

ANSI S1.43-1997 (R2002). 2002. Specifications for Integrating Averaging Sound Level Meters, American National Standards Institute, New York, NY.

Blevins, Robert D. 2001. *Flow-Induced Vibration*, Krieger Pub Co., Melbourne, FL, 2/e (reprint, 2001).

Bretthorst, G. Larry. 1988. *Bayesian Spectrum Analysis and Parameter Estimation*, Lecture Notes in Statistics Vol 48, Springer-Verlag, NY.

Graham, Paul. 2003. "Better Bayesian Filtering," http://www.paulgraham.com/better.html.

Hamernick, RP, Ahroon WA, Hsueh KD, Lei SF. 1993. Audiometric histological differences between the effects of continuous and impulse noise exposures. J. Acoust. Soc. Am. 93:20-88-2095.

Henderson, D, Hamernik RP. 1986. Impulse noise: a critical review. J. Acoust. Soc. Am. 80(2):569-584.

Kermani, Bahram G., Schiffman, Susan S., and Nagle, H.Troy. (2005). "Performance of the Levenberg-Marquardt neural network training method in electronic nose applications." Sensors and Actuators B 110, February 2005, pp. 13-22.

Kosko, Bart. 1992. *Neural Networks and Fuzzy Systems*, Prentice Hall, Englewood Cliffs, NJ

McKay, David. 1995. *Information Theory, Inference, and Learning Algorithms*, Cambridge University Press.

McQ, http://www.mcqassociates.com/products/noisewatch.php

Oles, LCOL. Gary. 2005. Marine Corps Base Camp Lejeune, personal communication.

Schomer, Paul, et al. 1994. "Human and Community Response to Military Sounds: Results from Field-Laboratory Tests of Small-arms, tracked-vehicle, and Blast Sounds," NCEJ, 42(2), pp. 71-84.

SERDP. 2003. Statement of Need #: CPSON-05-04, "Improved Methods and Monitoring Systems for Impulse Noise." (Broad Agency Announcement issued November 6, 2003).

Sivia, D. S. and J. Skilling. 2006, *Data Analysis: A Bayesian Tutorial*, Oxford University Press, Oxford, England, 2/e.

Vipperman, J.S., M.M Prince, A.M. Flamm, 2003. "Analysis of Impact Noise in a manufacturing setting in the evaluation of noise-induced hearing loss: Issues of Sampling and Instrumentation," (Invited Talk) NIOSH/NHCA Impulsive Noise: A NORA Hearing Loss Team Best Practice Workshop, Cincinnati, OH, May 8-9, 2003.

USACHPPM. 2005. "Range Sustainment and Encroachment," http://chppm-www.apgea.army.mil/dehe/morenoise/sustainment.aspx

Whiteford, David. 2005. USACHPPM 2005. Personal Communication.

Other Literature

ANSI S12.7-1986 (R1993). 1993. Methods for measurement of impulse noise. American National Standards Institute, New York, NY.

ANSI S12.17-1996. 1996. Impulse Sound Propagation for Environmental Noise Assessment, American National Standards Institute, New York, NY.

Cabell, R.H., Fuller, C.R. and O'Brien, W.F. 1992. "Identification of Helicopter Noise Using a Neural Network,"*AIAA Journal*, 30(3), pp.624-630.

Fidell, Sanford (editor). 1996. "Community Response to High-Energy Impulsive Sounds: An Assessment of the Field Since 1981," CHABA, National Research Council, National Academy of Sciences, Washington, DC.

MIL-STD-1474D. 1997. "Department of Defense Design Criteria Standards, Noise Limits" AMSC A7245.

Russell, William A. Jr., George A. Luz, *et al.* 2001. "Environmental Noise Management: An Orientation Handbook for Army Facilities," U.S. Army Center for Health Promotion and Preventive Medicine (USACHPPM).

Vipperman, J.S., 2003, "Active Noise Control Technology," (Invited Talk) State of the Art Concepts in Noise and Hearing Loss Conference, Pacific-Northwest Section of the American Industrial Hygiene Association, Seattle, Washington, October 15, 2003.

Appendix A. Supporting Data.

All useable data (noise recordings) that were collected in the field are being supplied on a DVD attached to this report. In addition, the MATLAB codes used to extract the signal metrics and train and test the ANN are supplied in the directory named "Matlab Codes." This report is in the "Report" directory and the summary of all signal metrics is given in ESLM_Signal_Metric_Outputs.xls in the directory "Data Summary." All waveform data in the form of text files are included in the directory "SERDP Library." Since this directory organizes the files by category into several subdirectories, Figure 20 graphically depicts of the structure of the "SERDP Library." At the bottom of leaf of each branch, each subdirectory is further divided into specific days and locations of each type of noise source that was recorded.
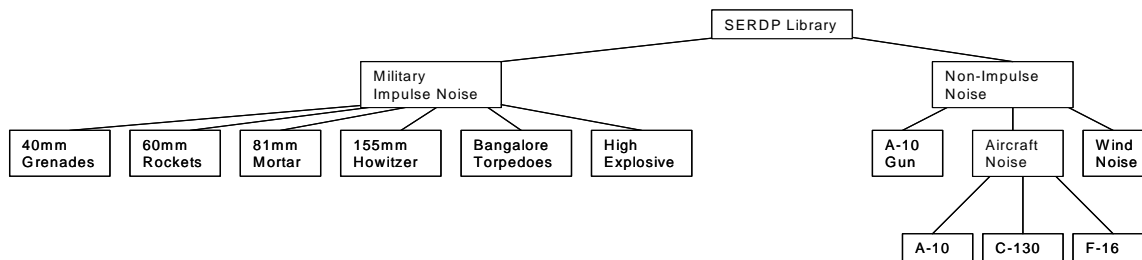

Figure 21: Directory Structure of supplied data DVD.

Appendix B. List of Technical Publications

<u>Published Abstract/Presentation:</u>

Vipperman, J. S., "Development of Metrics to Identify Military Impulse Noise,", 149th Meeting of the Acoustical Soc. of Am., Vancouver, BC Canada, May 16-20, 2005, also (abstract only) *J. Acoust. Soc. Am*. **117,** p. 2448.

Vipperman, J.S. and Brian Bucci, "Development of a Real-Time Military Noise Monitor," SERDP/ESTCP Partners in Environmental Technology Symposium and Workshop, Washington, DC, Nov. 29 – Dec. 1, 2005.

Bucci, Brian, Vipperman, J. S., "Development of Artificial Neural Network Classifier to Identify Military Impulse Noise," 151st Meeting of the Acoustical Soc. of Am., Providence, RI, June 5-9, 2006, accepted for presentation.

Conference Paper:

Bucci, Brian, Vipperman, J. S., "Artificial neural network military impulse noise classifier." IMECE2006-14065, Proceedings of IMECE 06: 2006 ASME International Mechanical Engineering Congress, November 5-10, 2006, Chicago, Illinois.

<u>Journal Paper:</u>

Bucci, Brian, Vipperman, J. S., "Development of an artificial neural network-based classifier to identify military impulse noise," In-Process. In Process, *J. Acoust. Soc. of Am.*